

The development of color histogram method to identify air quality index based on sky images

Sofika Enggari¹, Sumijan², Muhammad Tajuddin²

¹Department of Information System, Faculty of Computer Science, Universitas Putra Indonesia YPTK Padang, Padang, Indonesia

²Department of Doctoral Information Technology, Faculty of Computer Science, Universitas Putra Indonesia YPTK Padang, Padang, Indonesia

Article Info

Article history:

Received Nov 14, 2023

Revised Jan 8, 2024

Accepted Jan 19, 2024

Keywords:

Air quality index

Color histogram method

Identify air quality levels

ISPU mobile

Sky images

ABSTRACT

Air quality index measurements in Indonesia are carried out by ministry of environment and forestry (KLHK). The Ministry divides air quality levels into 5 categories, namely good, moderate, unhealthy, very unhealthy and dangerous. In this study, 3 air quality categories were used as primary research data, namely good, moderate and unhealthy because the others, never occurred in Indonesia from the time this research was conducted until its completion. This research develops the color histogram method in order to recognize the shape of an object in an image. First stage in this research is inputting the sky image into the system. Then carry out pre-processing in the form of cropping the image to obtained is only an image of sky. Next, convert the red, green and blue (RGB) colored sky image to Grayscale, then image enhancement, then noise reduction. After that is processed using development of the color histogram method. Refinement of color histogram method has yielded an impressive accuracy level of 90%, validated through the analysis of 30 sky images. The method successfully detected 27 images accurately, while three images posed detection challenges. The findings of this research is color histogram method can be used to identify objects especially air pollution from sky images.

This is an open access article under the [CC BY-SA](https://creativecommons.org/licenses/by-sa/4.0/) license.



Corresponding Author:

Sofika Enggari

Department of Information System, Faculty of Computer Science

Universitas Putra Indonesia YPTK Padang

Lubuk Begalung, Padang, West Sumatera, Indonesia

Email: sofika_enggari@upiptk.ac.id

1. INTRODUCTION

The air quality index (AQI) functions as a measure used to assess the degree of air pollution or the air quality in a specific location [1]–[3]. Typically, this measure is employed by governmental bodies to depict the condition of air quality within a particular area [4], [5]. Various countries around the world adopt different air quality indices, depending on the specified air quality standards inherent to each nation [6], [7]. In Indonesia, the responsibility for determining the air quality level lies with the Ministry of Environment and Forestry (KLHK) of the Republic of Indonesia (RI). The KLHK RI measures air particles smaller than 10 microns (micrometers), commonly known as particulates (PM10) [8]–[11]. The presence of these particulate elements can lead to complications in the respiratory system. Particles with a size less than 10 μm have the potential to enter the respiratory system. Those within the range of 5-10 μm can be effectively filtered by nasal cavity hair, particles within the range of 2-5 μm can penetrate the alveolus, while particles smaller than 2 μm can enter the respiratory system during inhalation and exit during exhalation. The levels of air pollution and their corresponding color indicators determined by the KLHK RI are outlined in Table 1.

Table 1. Air pollution index and color indicators

Range	Categories	Explanation
1-50	Good	The air quality index is very good, does not have a negative effect on humans, animals and plants
51-100	Medium	Air quality index are still acceptable for human, animal and plant health
101-200	Unhealthy	Air quality index that are detrimental to humans, animals and plants
201-300	Very unhealthy	Air quality index that can increase health risks in a number of exposed population segments
		Air quality levels that can seriously harm the health of the population and require immediate treatment

In accordance with the data presented in Table 1, KLHK RI has classified air quality into five categories, specifically: good, moderate, unhealthy, very unhealthy, and dangerous. The scope of the conducted research was confined to the analysis of three air quality categories, namely: healthy, moderate, and unhealthy. This limitation was imposed due to the prevailing air conditions in Indonesia throughout the duration of the research, which exclusively fell within the purview of these three aforementioned air quality categories. The remaining categories, namely very unhealthy and dangerous, were not observed during the entire course of the study. The assessment of the air pollution standard index (ISPU) [12]–[16] conducted by KLHK RI is presently facilitated through the utilization of the air quality monitoring system (AQMS) [17]–[21]. KLHK RI disseminates real-time ISPU measurement results via the internet, employing the ISPU Mobile application to provide accessible information.

The sky image examined in this study refers to a digital representation of the sky [22]–[24]. Subsequently, this digital portrayal of the sky undergoes processing to facilitate the detection of ISPU within the captured air depicted in the image [25], [26]. To validate the processed data in this study, a comparative analysis is carried out against the data presented by the mobile ISPU application provided by the Indonesian ministry of environment and forestry. The methodology formulated for conducting ISPU measurements on sky images is the color histogram method. This specific approach is well-suited for understanding and analyzing color digital images, utilizing mathematical calculations to ascertain the values of the color histogram within the image to ensure low Turnitin similarity test results.

Previous investigations supporting the aforementioned conditions encompass the research by Chuchro *et al.* [27], which delved into the utilization of photo texture analysis and weather data to evaluate air quality in relation to airborne PM10 and PM2.5 particulates. This study employed a texture analysis approach for each photo frame, and the results were employed in constructing regression and classification models. The outcomes of this study imply that the developed classification model is suitable for evaluating PM10 and PM2.5 air quality. Another inquiry conducted by Samsami *et al.* [28] explored the categorization of air quality levels based on the scrutiny of sky images. This investigation utilized image analytical techniques and computer vision methods by extracting image features. The results of this study indicate the accurate classification ability of the proposed method. Additionally, Vahdatpour *et al.* [29] conducted research in, focusing on air pollution forecasting from sky images using both shallow and deep classifiers. Employing two approaches, namely a method for estimating air pollution levels and a CNN method, the research demonstrated that the proposed method in the first approach achieved satisfactory accuracy in detecting air pollution levels, aiming to avoid high Turnitin similarity test results. This study aims to advance the color histogram method for extracting features from sky images based on color. Consequently, specific indicators are derived from the outcomes of feature extraction, facilitating the determination of whether the air quality or pollution level during image capture falls under the categories of Good, Moderate, or Unhealthy. The significance of this research lies in its potential to empower individuals in assessing air quality or pollution levels through the use of a digital or smartphone camera. The results of this study offer practical benefits to individuals interested in evaluating air pollution levels through sky images. Furthermore, they contribute to aiding the KLHK RI, local Provincial or City Environmental Services (DLH), and the general public in determining the values of the ISPU, aiming to mitigate the risk of high Turnitin similarity test results.

2. METHOD

2.1. Research framework

This sub-chapter explains in detail the process of developing the color histogram method so that this method is able to detect objects in the form of dust particles in the air of the PM 2.5 and PM 10 types in sky images. The results of this research were implemented in the form of a very practical and easy to use computer application, which provides unlimited access for the general public and KLHK RI. In Figure 1, you can see several stages summarized in one sketch, namely the research framework.

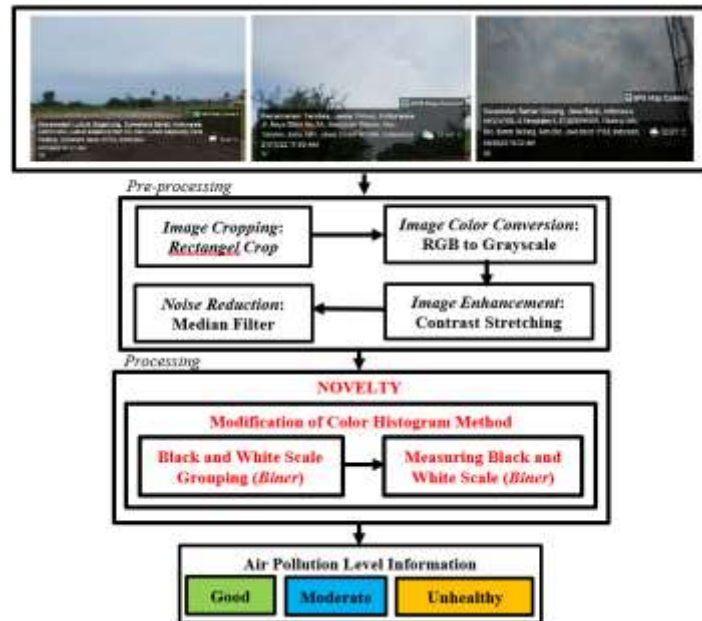


Figure 1. Research framework

2.2. Research framework details

2.2.1. Input stages (image collection)

This image compilation comprises original images utilized as input data, all in *.jpg format. The input images are color images with a pixel size of 1080×1350 pixels, and for this study, six sky images were selected, divided into three categories: two images representing good air quality, two images depicting moderate air quality, and two images illustrating unhealthy air quality. The process of capturing sky images involves on-site photography of the sky's atmospheric conditions using a cellphone camera, specifically the Samsung S23 Ultra model. This was conducted in three distinct regions of Indonesia. The first location chosen for capturing sky images with good air quality is Lubuk Begalung District, Padang City, West Sumatra. The second location, selected for capturing sky images illustrating moderate air quality, is Tandes District, Surabaya City, East Java. The third area where sky imagery was documented is Bandar Gebang District, Bekasi City, West Java. The aim is to minimize Turnitin similarity test results.

2.2.2. Pre-process stages

The pre-processing stage is a preliminary phase conducted prior to the main research stage [30], [31]. In this research, the pre-processing stage is segmented into four components [32], [33]. Firstly, there is the image cropping pre-processing, employing a rectangular cropping technique. Secondly, there is the pre-processing of image color conversion, transitioning from RGB color images to Grayscale images. The third pre-processing step involves enhancing image quality through the contrast stretching method. Lastly, the fourth pre-processing step focuses on noise reduction, utilizing the median filter method.

A. Image cropping: rectangle crop

At this stage of the research, image cropping is conducted by extracting or isolating a portion of a sky image frame that has been input into the system. In this initial pre-processing phase, the image cropping process is executed by isolating specific segments of the image to generate an image tailored to the user's or researcher's preferences for subsequent image processing. This specific cropping method is selected due to its capability to form a minimum of three sides and an unlimited number of sides based on the chosen coordinates.

B. Image color conversion: RGB to grayscale

The input image takes the form of a sky image that has undergone the rectangle crop technique, focusing only on a specific portion of the sky. Subsequently, the researchers proceeded to the second pre-processing stage, involving the conversion of the initially RGB-colored sky image into a grayscale representation. The formula utilized for this RGB to grayscale conversion is as (1):

$$y = 0,299 * R + 0,587 * G + 0,144 * B \quad (1)$$

Information: y = gray image pixel value, R = red image pixel value, G = green image pixel value, B = blue image pixel value.

C. Image enhancement: contrast stretching

The grayscale sky image resulting from the RGB to grayscale conversion mentioned earlier underwent a subsequent stage, where the researchers engaged in the process of enhancing image quality. This constitutes the third pre-processing stage, aimed at maximizing the grayscale extension of the sky image and eliminating noise. In the contrast stretching method, each pixel in image undergoes transformation using the following function:

$$b(i, j) = \frac{a(i, j)}{d-c} (L - 1) \quad (2)$$

Information: $b(i, j)$ = image pixel after transformation, $a(i, j)$ = image pixel before transformation, c = maximum value of the input image, d = minimum value of the input image, L = maximum pixel value, namely 255.

D. Noise reduction: median filter

Following the enhancement of the sky image quality through the contrast stretching method as mentioned, the researchers proceeded with the image noise reduction process. The method employed for reducing image noise is the median filter method, a non-linear technique commonly employed to mitigate salt and pepper types of noise. The formula employed in the median filter method is:

$$f(x, y) = \text{median} \sum(s, t) * S_{x,y} * g(s, t) \quad (3)$$

Information: $f(x, y)$ = new image pixel value after noise reduction, $\text{median} \sum(s, t)$ = median value of the entire image, $S_{x,y}$ = window area covered by the filter, $g(s, t)$ = sub image $S_{-}(x, y)$.

2.2.3. Processing stages

A. Old color histogram method

The next stage is processing, namely implementing the color histogram method. Currently the color histogram method is only able to measure the histogram values of all the colors of an image. The formula used to implement the old color histogram method:

$$P(c) = \frac{N(c)}{M} \quad (4)$$

Information: $P(c)$: probability first order histogram, $N(c)$: pixel value of image channel c , M : number of pixels in an image. Formula 4 is implemented in the form of pseudocode 4 which is a coding program for the old color histogram method using the MATLAB programming language. The pseudocode 1 presented in this research.

Pseudocode 1. Old color histogram method

Input:

```
myhist=zeros(256,1);
for k=0 : 255
myhist(k+1)=numel(find(F==k));
number of elements where F has gray level equal to 'k'
end
```

Output:

```
imshow(F); title('Histogram of Original Image');
```

Initialization:

```
cdf=zeros(256,1); cdf(1)=myhist(1); for k=2 : 256 cdf(k)=cdf(k-1)+myhist(k);
end
cumprob=cdf/(rows.*cols); equalizedhist=floor((cumprob).*255);
cumprob=cdf/(rows.*cols); equalizedhist=floor((cumprob).*255);
for i=1 : cols
for j=1 : rows
for m = 0 : 255 %if(F(i,j)==m) %G(i,j)=equalizedhist(m+1); %end
end
end
end
end
myeqhist=zeros(256,1); for k=0 : 255 myeqhist(k+1)=numel(find(G==k));
end
```

B. The development of color histogram method

In this research, modifications were introduced to the color histogram method. Presently, the color histogram method solely assesses the histogram values of all the colors within an image. Addressing the aforementioned challenge, researchers devised an enhanced color histogram method tailored for application with sky images, specifically for the detection of airborne dust particles based on such imagery. The ensuing formula illustrates the implementation of this novel color histogram method:

$$P(c) = \frac{\frac{N(c1) \times 10}{N(c2) \times 2,5}}{M} \quad (5)$$

Information: P(c): probability process order histogram, N(c1): floor pixel value of channel 1 image c, N(c2): floor pixel value of channel 1 image c, M : number of pixels in an image. Formula 5 is implemented in the form of pseudocode 2 which is a coding program for the old color histogram method using the MATLAB programming language. The pseudocode 2 presented in this research.

Pseudocode 2. The development of color histogram method

Input:

```
myhist=zeros(256,1); for k=0 : 255 myhist(k+1)=numel(find(F==k)); end
```

Output:

```
imshow(F); title('Histogram of Original Image ');
```

Initialization:

```
cdf=zeros(256,1); cdf(1)=myhist(1); for k=2 : 256 cdf(k)=cdf(k-1)+myhist(k); end
```

```
J = I;
```

```
cumprob = cdf/(rows.*cols); equalizedhist1 = floor((cumprob).*10);
```

```
equalizedhist2 = floor((cumprob).*2.5);
```

```
for i=1 : cols
```

```
for j=1 : rows
```

```
for m = 0 : 255
```

```
if(F(i,j)==m) %G(i,j)=equalizedhist(m+1);%end
```

```
end
```

```
end
```

```
myeqhist=zeros(256,1); for k=0 : 255 myeqhist(k+1)=numel(find(G==k));
```

end

3. RESULTS AND DISCUSSION

3.1. Result of input stages (image collection)

This image collection contains original images that are used as input data. The image used as input image is a sky image in the form of a file in *.jpg format. The test images in this research comprise six sky images categorized into three types. Figure 2 provides visual examples of the different sky images. Two images represent the sky under good air quality conditions, as illustrated in Figure 2(a). Additionally, two images depict the sky under moderate air quality conditions, as shown in Figure 2(b). Finally, two images showcase the sky under unhealthy air quality conditions, presented in Figure 2(c).



Figure 2. Sky image; (a) good air quality, (b) moderate air quality, and (c) unhealthy air quality

3.2. Result of pre-process stages

The preprocessing stages in this research are categorized into three sequential phases. Firstly, image cropping is performed, followed by the conversion of color images from RGB to grayscale. Secondly, image enhancement is conducted utilizing the contrast stretching method. Lastly, noise reduction is executed through the application of the median filter method.

3.2.1. Result of image cropping: rectangle crop

In this research, the pre-processing step of image cropping is conducted using a rectangle cropping method. This technique involves cropping connected coordinate points in a rectangular shape. The position of the rectangle for cropping in the sky image corresponds to the location from which the sky image will be extracted. The outcomes of this pre-processing, particularly the cropped images, are illustrated in Figure 3. Figure 3(a) represents the cropped image from an instance of good air quality, Figure 3(b) depicts the cropped image from a moderate air quality scenario, and Figure 3(c) displays the cropped image from an unhealthy air quality situation.

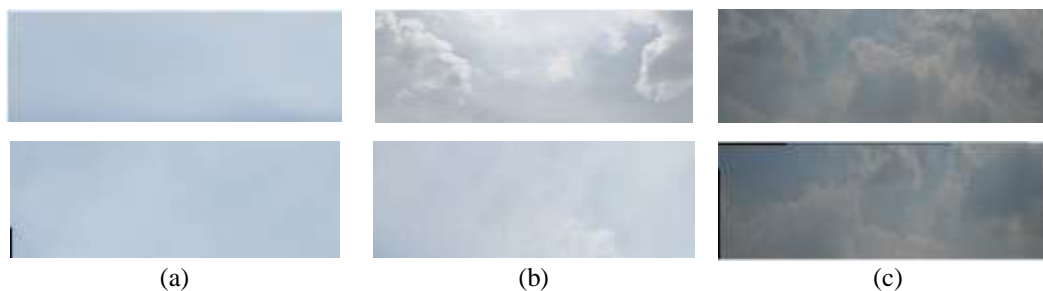


Figure 3. Result of image cropping sky image from; (a) good, (b) moderate, and (c) unhealthy, air quality

3.2.2. Image color conversion: RGB to Grayscale

The input image in this study is a selectively cropped sky image using the rectangle crop technique, focusing on a specific sky section. Subsequently, the researchers proceeded with the second pre-processing stage, involving the conversion of the sky image from its initial RGB color format to grayscale. In this pre-processing step, each RGB-colored image pixel undergoes conversion to a grayscale image with varying gray levels contingent on the previous RGB-colored pixel's value. Darker colors yield darker gray shades, while lighter colors result in lighter gray tones. The outcomes of this pre-processing, particularly the color conversion, are illustrated in Figure 4. Figure 4(a) illustrates the color-converted image from the cropped image of good air quality (Figure 3(a)), Figure 4(b) shows the color-converted image from the cropped image of moderate air quality (Figure 3(b)), and Figure 4(c) displays the color-converted image from the cropped image of unhealthy air quality (Figure 3(c)).

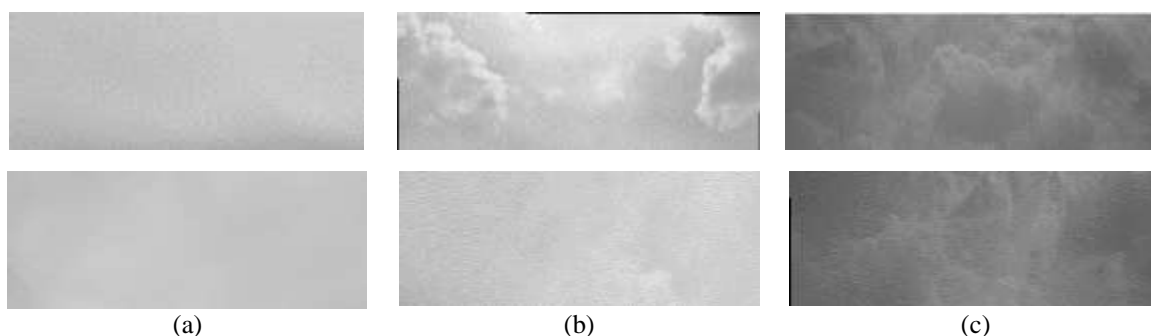


Figure 4. Result of color conversion sky image; (a) good, (b) moderate, and (c) unhealthy, air quality

3.2.3. Image enhancement: contrast stretching

The sky image, having undergone the conversion from RGB color to grayscale as previously mentioned, prompted researchers to initiate the process of enhancing image quality. This constitutes the third

pre-processing stage, specifically aimed at maximizing the grayscale extension of the sky image while mitigating noise. The selected method for improving image quality is the contrast stretching method. This technique proves effective in elevating the quality of digital images concerning illumination, achieved by fine-tuning the brightness and contrast levels. These adjustments render the image suitable for subsequent pre-processing stages. In the contrast stretching method, each pixel in image A undergoes a transformation. The outcomes of this pre-processing, particularly the image enhancement, are illustrated in Figure 5. Figure 5(a) illustrates the image enhancement from the color conversion image of good air quality (Figure 4(a)), Figure 5(b) shows the image enhancement from the color conversion image of moderate air quality (Figure 4(b)), and Figure 5(c) displays the image enhancement from the color conversion image of unhealthy air quality (Figure 4(c)).

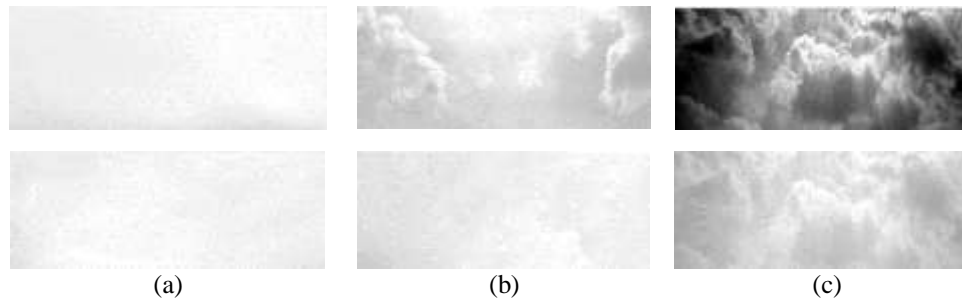


Figure 5. Result of image enhancement from sky image; (a) good, (b) moderate, and (c) unhealthy, air quality

3.2.4. Noise reduction: median filter

The enhancement of sky image quality through the contrast stretching method, as aforementioned, marks the subsequent undertaking by researchers in the process-image noise reduction. This constitutes the fourth pre-processing stage, dedicated to mitigating disturbances in the processed image, ensuring clarity and precision aligned with the intended examination. The method employed for reducing image noise is the median filter method, recognized for its non-linear attributes and frequent application in mitigating salt and pepper noise types. The technique involves substituting each pixel value with the median value of adjacent pixel values within a designated window. The median value is derived by sorting all pixel values within the window, subsequently replacing pixel values throughout the image with the median pixel value. The outcomes of this pre-processing, particularly the noise reduction, in Figure 6. Figure 6(a) illustrates the noise reduction image from the image enhancement of good air quality (Figure 5(a)), Figure 6(b) shows the noise reduction image from the image enhancement of moderate air quality (Figure 5(b)), and Figure 6(c) displays the noise reduction image from the image enhancement of unhealthy air quality (Figure 5(c)).

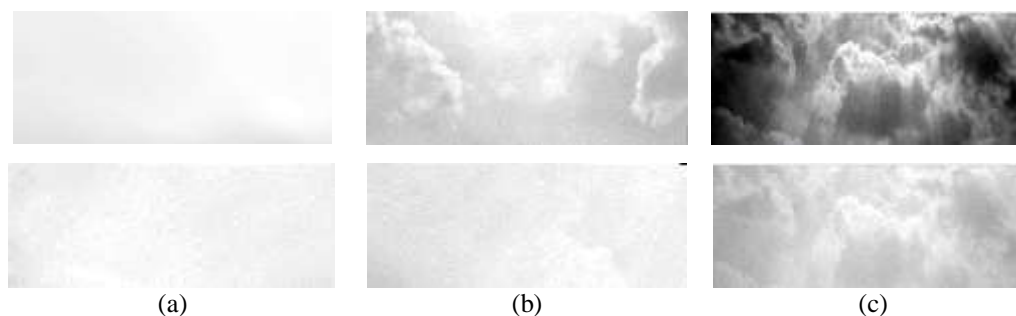


Figure 6. Result of noise reduction from sky image; (a) good, (b) moderate, and (c) unhealthy, air quality

3.3. Processing stages

3.3.1. Old color histogram method

The color histogram method is employed for quantifying the color histogram value of an image. This research was undertaken to assess the air quality levels depicted in sky images. The measurement of air

quality levels is conducted through the utilization of the color histogram method, providing precise insights into the air quality level based on the sky image. The outcomes of this pre-processing, particularly the old color histogram method, are illustrated in Figure 7. Figure 7(a) illustrates the old color histogram method from the noise reduction image of good air quality (Figure 6(a)), Figure 7(b) shows the old color histogram method from the noise reduction image of moderate air quality (Figure 6(b)), and Figure 7(c) displays the old color histogram method from the noise reduction image of unhealthy air quality (Figure 6(c)).

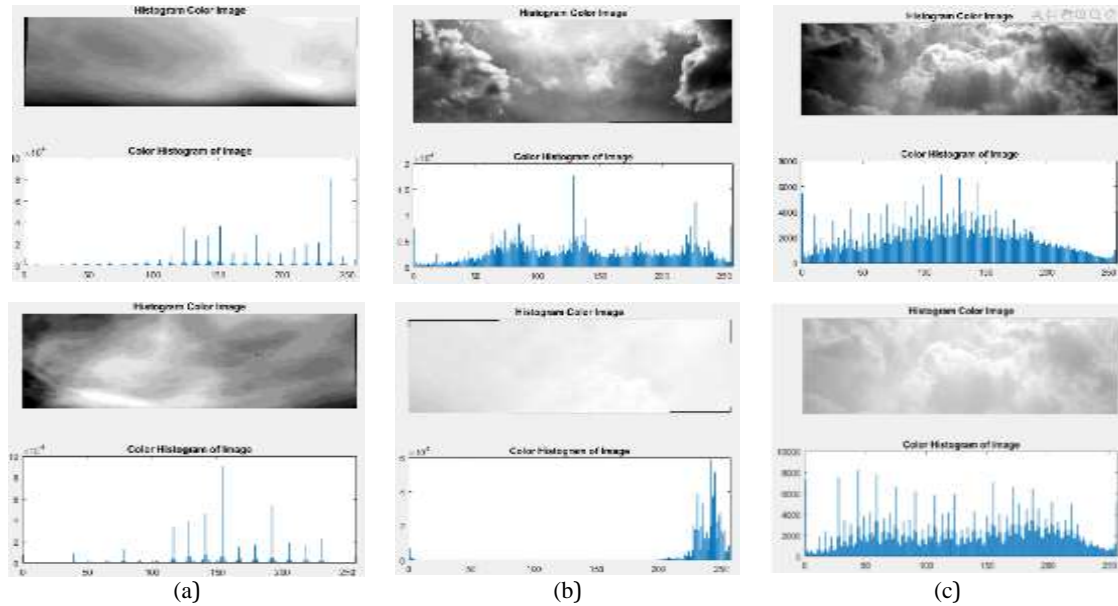


Figure 7. Result of old color histogram method; (a) good, (b) moderate, and (c) unhealthy, air quality

In the Figure 7, the image represents the outcome of the color histogram method. The upper image serves as a visual representation of the color histogram method, while the lower image presents a graphical representation of the color histogram values derived from the sky image. However, the conventional color histogram method remains incapable of quantifying the extent of air pollution in the sky image. Additionally, it fails to discern the specific air quality level at the time the sky image was captured.

3.3.2. The development of color histogram method

The evolution of the conventional color histogram method into an advanced variant is imperative to facilitate a clear visual distinction between air pollution and non-air pollution based on sky images. The conventional color histogram method’s efficacy in measuring air quality levels from sky images remains suboptimal, lacking clarity in distinguishing images depicting air pollution from those that do not. In contrast, the refined color histogram method offers enhanced clarity. Figure 8 illustrates the outcomes of this methodological advancement. The outcomes of this pre-processing, particularly the development color histogram method, are illustrated in Figure 8. Figure 8(a) illustrates the development color histogram method from the noise reduction image of good air quality (Figure 6(a)), Figure 8(b) shows the development color histogram method from the noise reduction image of moderate air quality (Figure 6(b)), and Figure 8(c) displays the development color histogram method from the noise reduction image of unhealthy air quality (Figure 6(c)).

In Figure 8 you can see the image resulting from the new color histogram method. The image in Figure 7 is a visual form of the new color histogram method where the difference between the image of a clean sky and dust particles is clearly visible. The white image is dust particles or air pollution, while the black image is an image of a clean sky. The image in Figure 8 is a graphic form of the color histogram values measured from the sky image. Seen in the red line graph is the measured number of dust particles or air pollution. The old color histogram method is a method used to measure the histogram value in an image based on the color of the image. The weakness of the old color histogram method is the method’s inability to separate the histogram values of one color from the histogram values of other colors. In this research, it was successful in separating white color histogram values, which represents clean air without air pollution, and separating gray color histogram values, which represents air with polluted air. The novelty in this research is the development of the color histogram method from the old color histogram method to the new color histogram method. As is known so far, the histogram method cannot be used to recognize the shape of

objects in an image. This can be solved in this research, which is novel in this research, namely the color histogram method can be used to recognize the shape of objects. The results obtained after developing the color histogram method can be used to measure the number of fine PM 10 particles in the air based on sky images. Apart from that, you can also see visually which part of the sky image is dust or air pollution or which is clean air. In this research, to be able to produce an image like the one in the image Figure 7, we made modifications to the color histogram method formula. In Table 2 shows a comparison of the old color histogram formula with the new color histogram method formula.

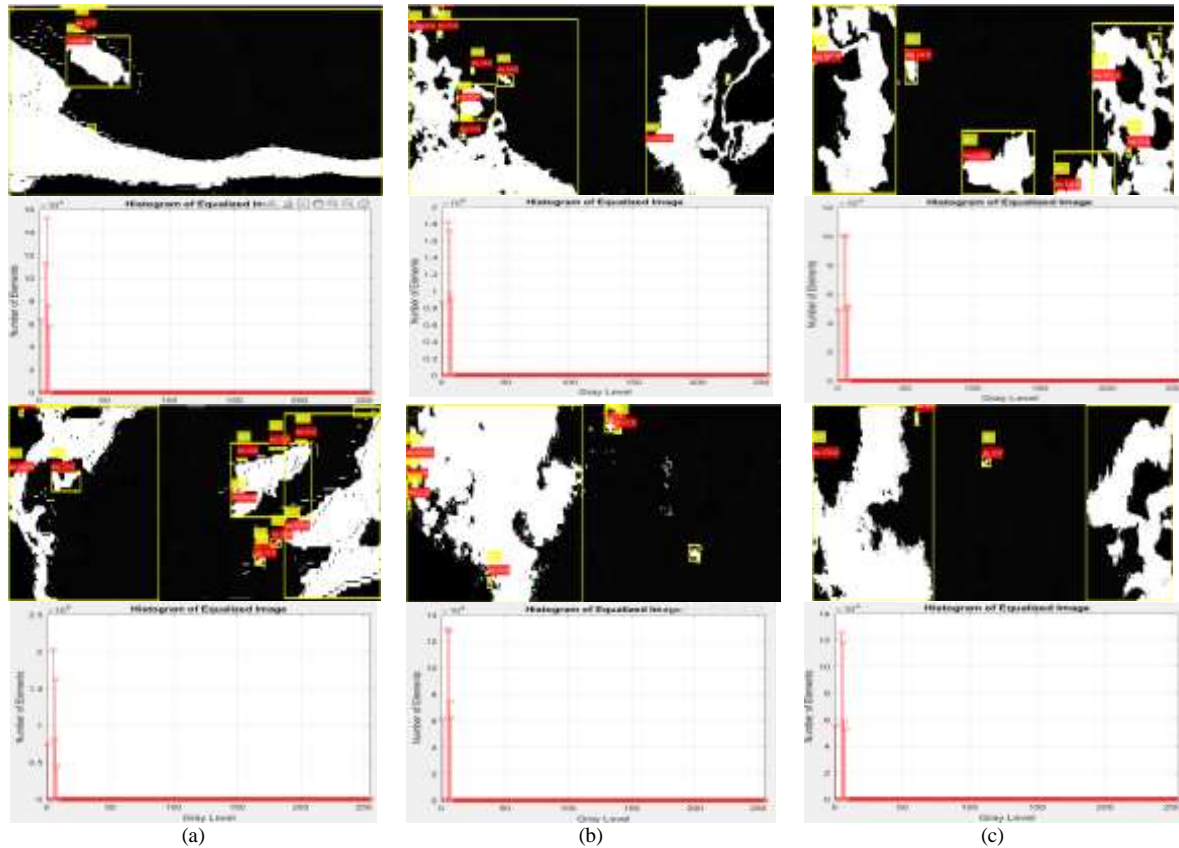


Figure 8. Result of development color histogram method from sky image; (a) good air quality, (b) moderate air quality, and (c) unhealthy air quality

Table 2. Comparison of formulas old color histogram method and new color histogram method

	Old color histogram method	Development color histogram method
	$P(c) = \frac{N(c)}{M}$	$P(c) = \frac{N(c1) \times 10}{N(c2) \times 2,5 \times M}$
Information:	P(c): Probability of first order histogram N(c): Image channel pixel value c	P(c): Probability of first order histogram N(c1): Image channel 1-pixel floor value c N(c2): Image channel 2-pixel floor value c
	M: The number of pixels in an image	M: The number of pixels in an image

The modification in the formula of the old color histogram method to the new color histogram formula involves the subdivision of the N(c) value into two distinct types, denoted as N(c1) and N(c2). The N(c1) value is ascribed to an image indicative of dust or pollution, whereas the N(c2) value is assigned to an image representing a clean environment free from dust or pollution. Subsequently, the N(c1) value undergoes multiplication by the factor 10, denoted as the 10 micron particulate value, while the N(c2) value is multiplied by the factor 2.5, known as the 2.5 particulate value. These particulate values correspond to the composition of air and can be visually discerned. Following this, the N(c1) value is divided by the N(c2) value, and the resulting quotient is further divided by the M value, representing the number of pixels in an image. Consequently, the outcomes yield measurements of air quality and a visual representation of air pollution.

4. CONCLUSION

This research introduces the development of a color histogram method, aptly named the color histogram method, designed to accurately identify air pollution levels based on sky images. The refinement of the color histogram method has yielded an impressive accuracy level of 90%, validated through the analysis of 30 sky images encompassing three distinct air quality categories. This dataset comprised 10 sky images representing good air quality, 10 depicting moderate air quality, and another 10 reflecting unhealthy air quality. The method successfully detected 27 images accurately, while three images posed detection challenges. These outcomes align with the measurements conducted by the Indonesian ministry of environment and forestry utilizing the AQMS tool, as well as the data presented on ISPU Mobile. It is important to note that the application developed in this research exclusively serves the purpose of identifying air quality levels and is not intended for the assessment of other objects' quality.





REFERENCES

- [1] Y. Li and R. Li, "A hybrid model for daily air quality index prediction and its performance in the face of impact effect of COVID-19 lockdown," *Process Safety and Environmental Protection*, vol. 176, pp. 673–684, Aug. 2023, doi: 10.1016/j.psep.2023.06.021.
- [2] N. N. Maltare and S. Vahora, "Air Quality Index prediction using machine learning for Ahmedabad city," *Digital Chemical Engineering*, vol. 7, p. 100093, Jun. 2023, doi: 10.1016/j.dche.2023.100093.
- [3] Y. Wang, L. Huang, C. Huang, J. Hu, and M. Wang, "High-resolution modeling for criteria air pollutants and the associated air quality index in a metropolitan city," *Environment International*, vol. 172, p. 107752, Feb. 2023, doi: 10.1016/j.envint.2023.107752.
- [4] A. Dubey and A. Rasool, "Impact on air quality index of india due to lockdown," *Procedia Computer Science*, vol. 218, pp. 969–978, 2022, doi: 10.1016/j.procs.2023.01.077.
- [5] D. P. Shah and D. P. Patel, "A comparison between national air quality index, india and composite air quality index for Ahmedabad, India," *Environmental Challenges*, vol. 5, p. 100356, Dec. 2021, doi: 10.1016/j.envc.2021.100356.
- [6] P. L. Fung *et al.*, "Improving the current air quality index with new particulate indicators using a robust statistical approach," *Science of the Total Environment*, vol. 844, p. 157099, Oct. 2022, doi: 10.1016/j.scitotenv.2022.157099.
- [7] N. Das, S. Sutradhar, R. Ghosh, and P. Mondal, "Asymmetric nexus between air quality index and nationwide lockdown for COVID-19 pandemic in a part of Kolkata metropolitan, India," *Urban Climate*, vol. 36, p. 100789, Mar. 2021, doi: 10.1016/j.uclim.2021.100789.
- [8] R. G. A. Politek, S. He, P. F. C. Wilms, J. K. Keppler, M. E. Bruins, and M. A. I. Schutyser, "Effect of relative humidity on milling and air classification explained by particle dispersion and flowability," *Journal of Food Engineering*, vol. 358, p. 111663, Dec. 2023, doi: 10.1016/j.jfoodeng.2023.111663.
- [9] K. Liu *et al.*, "Gas-particle partitioning of organophosphate esters in indoor and outdoor air and its implications for individual exposure," *Environment International*, vol. 181, p. 108254, Nov. 2023, doi: 10.1016/j.envint.2023.108254.
- [10] Y. Zhou and L. Jiang, "Identification of swirling air flow velocity by non-neutrally buoyant tracer particle based on machine learning," *Flow Measurement and Instrumentation*, vol. 91, p. 102363, Jun. 2023, doi: 10.1016/j.flowmeasinst.2023.102363.
- [11] N. Fu, M. K. Kim, L. Huang, J. Liu, B. Chen, and S. Sharples, "Investigating the reliability of estimating real-time air exchange rates in a building by using airborne particles, including PM1.0, PM2.5, and PM10: a case study in Suzhou, China," *Atmospheric Pollution Research*, vol. 15, no. 1, p. 101955, Jan. 2024, doi: 10.1016/j.apr.2023.101955.
- [12] D. K. Jigyasu *et al.*, "Air pollution tolerance index of *Persea bombycina*: primary food plant of endemic muga silkworm (*Antheraea assamensis*)," *Heliyon*, vol. 9, no. 11, p. e21184, Nov. 2023, doi: 10.1016/j.heliyon.2023.e21184.
- [13] S. Shahrukh *et al.*, "Air pollution tolerance, anticipated performance, and metal accumulation indices of four evergreen tree species in Dhaka, Bangladesh," *Current Plant Biology*, vol. 35–36, p. 100296, Sep. 2023, doi: 10.1016/j.cpb.2023.100296.
- [14] S. Warkentin *et al.*, "Changes in air pollution exposure after residential relocation and body mass index in children and adolescents: a natural experiment study," *Environmental Pollution*, vol. 334, p. 122217, Oct. 2023, doi: 10.1016/j.envpol.2023.122217.
- [15] S. Xu *et al.*, "Long-term exposure to low-level air pollution and greenness and mortality in Northern Europe. The Life-GAP project," *Environment International*, vol. 181, p. 108257, Nov. 2023, doi: 10.1016/j.envint.2023.108257.
- [16] M. Shehzad, A. Younis, M. Asif, and M. Hameed, "Prospects of green roof technology as a sustainable solution to urban pollution index," *Journal of Agriculture and Food Research*, vol. 14, p. 100751, Dec. 2023, doi: 10.1016/j.jafr.2023.100751.
- [17] J. H. Buelvas, D. Múnera, and N. Gaviria, "DQ-MAN: A tool for multi-dimensional data quality analysis in IoT-based air quality monitoring systems," *Internet of Things (Netherlands)*, vol. 22, p. 100769, Jul. 2023, doi: 10.1016/j.iot.2023.100769.
- [18] D. N. Paithankar, A. R. Pabale, R. V. Kolhe, P. William, and P. M. Yawalkar, "Framework for implementing air quality monitoring system using LPWA-based IoT technique," *Measurement: Sensors*, vol. 26, p. 100709, Apr. 2023, doi: 10.1016/j.measen.2023.100709.
- [19] N. S. Gupta, Y. Mohta, K. Heda, R. Armaan, B. Valarmathi, and G. Arulkumaran, "Prediction of air quality index using machine learning techniques: a comparative analysis," *Journal of Environmental and Public Health*, vol. 2023, pp. 1–26, Jan. 2023, doi: 10.1155/2023/4916267.
- [20] G. Shen, S. Ye, S. Shen, Y. Xu, and H. Shang, "Quality data collection and quality monitoring of smart electric energy meter based on acceleration sensor," *Journal of Sensors*, vol. 2022, pp. 1–10, Jun. 2022, doi: 10.1155/2022/7583712.
- [21] H. Dai, D. Huang, and H. Mao, "A Monitoring system for air quality and soil environment in mining areas based on the internet of things," *Journal of Sensors*, vol. 2022, pp. 1–7, Aug. 2022, doi: 10.1155/2022/5419167.
- [22] G. Terrén-Serrano and M. Martínez-Ramón, "Processing of global solar irradiance and ground-based infrared sky images for solar nowcasting and intra-hour forecasting applications," *Solar Energy*, vol. 264, p. 111968, Nov. 2023, doi: 10.1016/j.solener.2023.111968.
- [23] Q. Paletta, G. Arbod, and J. Lasenby, "Omnivision forecasting: combining satellite and sky images for improved deterministic and probabilistic intra-hour solar energy predictions," *Applied Energy*, vol. 336, p. 120818, Apr. 2023, doi: 10.1016/j.apenergy.2023.120818.
- [24] L. Zhang, R. Wilson, M. Sumner, and Y. Wu, "Advanced multimodal fusion method for very short-term solar irradiance forecasting using sky images and meteorological data: A gate and transformer mechanism approach," *Renewable Energy*, vol. 216, p. 118952, Nov. 2023, doi: 10.1016/j.renene.2023.118952.





- [25] P. Manandhar, M. Temimi, and Z. Aung, "Short-term solar radiation forecast using total sky imager via transfer learning," *Energy Reports*, vol. 9, pp. 819–828, Mar. 2023, doi: 10.1016/j.egy.2022.11.087.
- [26] H. Zhang, H. Tang, and W. Zhang, "Aurora retrieval in all-sky images based on hash vision transformer," *Heliyon*, vol. 9, no. 10, p. e20609, Oct. 2023, doi: 10.1016/j.heliyon.2023.e20609.
- [27] M. Chuchro, W. Sarlej, M. Grzegorzcyk, and K. Nurzyńska, "Application of photo texture analysis and weather data in assessment of air quality in terms of airborne PM10 and PM2.5 particulate matter," *Sensors*, vol. 21, no. 16, p. 5483, Aug. 2021, doi: 10.3390/s21165483.
- [28] M. M. Samsami, N. Shojaei, S. Savar, and M. Yazdi, "Classification of the air quality level based on analysis of the sky images," in *ICEE 2019 - 27th Iranian Conference on Electrical Engineering*, Apr. 2019, pp. 1492–1497, doi: 10.1109/IranianCEE.2019.8786738.
- [29] M. S. Vahdatpour, H. Sajedi, and F. Ramezani, "Air pollution forecasting from sky images with shallow and deep classifiers," *Earth Science Informatics*, vol. 11, no. 3, pp. 413–422, Sep. 2018, doi: 10.1007/s12145-018-0334-x.
- [30] Y. Jiang, B. Benatallah, and M. Báez, "Understanding how early-stage researchers leverage socio-technical affordances for distributed research support," *Information and Software Technology*, vol. 165, p. 107340, Jan. 2024, doi: 10.1016/j.infsof.2023.107340.
- [31] V. P. Lobanov, J. Pate, and J. Joyce, "Sturgeon and paddlefish: Review of research on broodstock and early life stage management," *Aquaculture and Fisheries*, May 2023, doi: 10.1016/j.aaf.2023.04.001.
- [32] H. Hendri, S. Enggari, Mardison, M. R. Putra, and L. N. Rani, "Automatic system to fish feeder and water turbidity detector using arduino mega," *Journal of Physics: Conference Series*, vol. 1339, no. 1, p. 012013, Dec. 2019, doi: 10.1088/1742-6596/1339/1/012013.
- [33] H. Hendri, Masriadi, and Mardison, "A novel algorithm for monitoring field data collection officers of Indonesia's Central statistics agency (BPS) using web-based digital technology," *International Journal on Advanced Science, Engineering and Information Technology*, vol. 13, no. 3, pp. 1154–1162, Jun. 2023, doi: 10.18517/ijaseit.13.3.18302.

BIOGRAPHIES OF AUTHORS







Sofika Enggari     is a dedicated lecturer in the Information System Study Program within the Faculty of Computer Science at Universitas Putra Indonesia YPTK Padang, Sumatera Barat, Indonesia. He earned his Bachelor's Degree and Master Degree from Universitas Putra Indonesia YPTK Padang in the Information System program under the Faculty of Computer Science. Currently, Enggari is engaged in doctoral studies at Universitas Putra Indonesia YPTK Padang, focusing on Information Technology within the Computer Science Faculty. Enggari unique identifier. His research endeavors traverse diverse domains, with particular expertise in image processing, information system, and web design. Sofika Enggari welcomes communication and collaboration. He can be contacted at email: sofika_enggari@upiyptk.ac.id.



Sumijan     is a dedicated lecturer and Associate Professor in the Information Technology (S3) Study Program within the Faculty of Computer Science at Universitas Putra Indonesia YPTK Padang, Indonesia. He earned his Bachelor's Degree from Universitas Putra Indonesia YPTK Padang in the Information System program under the Faculty of Computer Science. Subsequently, he pursued a Master's Degree at University Technology Malaysia (UTM). And he pursued a doctoral degree from Gunadarma University. Currently, Sumijan is Vice Rector I from Universitas Putra Indonesia YPTK Padang. Sumijan unique identifier. His research endeavors traverse diverse domains, with particular expertise in image processing, information system, and web design. Sumijan welcomes communication and collaboration. He can be contacted at email: sumijan@upiyptk.ac.id.



Muhammad Tajuddin     is a dedicated lecturer and Professor in the Information Technology (S3) Study Program within the Faculty of Computer Science at Universitas Putra Indonesia YPTK Padang, Sumatera Barat, Indonesia. He earned his Bachelor's Degree from Universitas Mataram in the Information System program under the Faculty of Computer Science. Subsequently, he pursued a Master's Degree at Universitas Brawijaya, specializing in Computer Science. And he pursued a doctoral degree from Universitas Brawijaya. His academic pursuits reflect a commitment to continuous learning and scholarly excellence. Muhammad tajuddin unique identifier. His research endeavors traverse diverse domains, with particular expertise in image processing, information system, and web design. Muhammad Tajuddin welcomes communication and collaboration. He can be contacted at email: tajuddin@universitasbumigora.ac.id.